eISSN (Online): 2598-0580

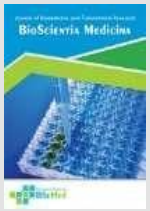

Bioscientia Medicina: Journal of Biomedicine & Translational Research

Journal Homepage: www.bioscmed.com

Dose- and Time-Dependent Efficacy of Topical Hydroquinone in Establishing a C57BL/6 Mouse Model of Vitiligo

Benedikta Lauda[1*], Nurrachmat Mulianto[1], Endra Yustin Ellistasari[1], Muhammad Eko Irawanto[1]

[1]Department of Dermatology and Venereology, Faculty of Medicine, Universitas Sebelas Maret/Dr. Moewardi Regional General Hospital, Surakarta, Indonesia

ARTICLE INFO

Keywords:
Animal model
C57BL/6 mice
Depigmentation
Hydroquinone
Vitiligo

***Corresponding author:**
Benedikta Lauda

E-mail address:
benelauda11@gmail.com

All authors have reviewed and approved the final version of the manuscript.

https://doi.org/10.37275/bsm.v10i1.1481

A B S T R A C T

Background: Vitiligo is a complex autoimmune depigmenting disorder driven by melanocyte-specific CD8+ T cells, oxidative stress, and genetic susceptibility. The lack of standardized, accessible animal models that recapitulate these pathways hinders therapeutic development. This study aimed to systematically optimize and validate a chemically-induced vitiligo model in C57BL/6 mice. **Methods:** Eighty (80) male C57BL/6 mice were randomized into ten groups (n=8/group). Experimental groups received once-daily topical applications of hydroquinone (HQ) at 2.5%, 5%, or 10%, or monobenzone (MBZ) at 40% for 8 or 16 days. Vehicle-treated mice served as controls. Efficacy was assessed via quantitative histopathology (Masson-Fontana staining for melanin area), biomolecular assays for oxidative stress (Malondialdehyde [MDA] and Superoxide Dismutase [SOD]), and RT-qPCR for melanogenesis-related (Tyr) and inflammation-related (Tnf) gene expression. **Results:** A clear dose- and time-dependent depigmentation was observed. The 10% HQ 16-day protocol was maximally effective, inducing a profound reduction in epidermal melanin area (0.06 ± 0.02) compared to 16-day controls (0.40 ± 0.04; $p < 0.001$). This histopathological finding was significantly correlated with severe cutaneous oxidative stress, evidenced by a 3.75-fold increase in MDA ($p < 0.001$) and a 50% reduction in SOD activity ($p < 0.001$) versus controls. Furthermore, this regimen caused a potent suppression of Tyr expression (0.15-fold change; $p < 0.001$) and a significant upregulation of the pro-inflammatory cytokine Tnf (3.8-fold change; $p < 0.001$). **Conclusion:** The 16-day topical application of 10% hydroquinone is a reliable, rapid, and highly reproducible protocol for inducing vitiligo-like depigmentation in C57BL/6 mice. This model successfully recapitulates key pathophysiological pillars of human vitiligo, including melanocytotoxicity, profound oxidative stress, and a pro-inflammatory cutaneous environment, establishing it as a valuable platform for preclinical therapeutic screening.

1. Introduction

Vitiligo is an acquired, chronic depigmenting disorder of the skin and hair, characterized by the progressive loss of functional melanocytes from the epidermis. It presents clinically as well-demarcated, milky-white macules and patches that can be aesthetically disfiguring and carry a profound psychosocial burden, significantly impairing quality of life and inducing social stigma, anxiety, and depression.[1] With a global prevalence estimated between 0.5% and 2.0%, vitiligo is the most common depigmenting disorder, affecting individuals of all races and skin types.[2]

The etiopathogenesis of vitiligo is complex and multifactorial, best understood through a "convergence hypothesis" where genetic predisposition, environmental triggers, metabolic dysfunction, and cellular stress converge to incite an autoimmune attack.[3] The dominant mechanism in non-segmental vitiligo, the most common form, is unequivocally autoimmune. This process is mediated by a cascade of autoreactive, skin-resident CD8+ T

cells that recognize melanocyte differentiation antigens (such as MART-1, Tyrosinase, and gp100) and execute melanocyte killing.[4] This autoimmune axis is critically dependent on the IFN-γ/CXCL10 signaling pathway. IFN-γ secreted by T cells induces keratinocytes to produce CXCL10, which in turn recruits more pathogenic T cells to the skin, creating a destructive positive-feedback loop.

However, this autoimmune attack does not occur in a vacuum. Compelling evidence points to an intrinsic melanocyte vulnerability, particularly an impaired capacity to manage oxidative stress. Melanocytes from vitiligo patients, even in non-lesional skin, exhibit a pro-oxidant state characterized by elevated levels of reactive oxygen species (ROS) and reduced levels of antioxidants such as catalase, glutathione peroxidase, and superoxide dismutase (SOD). Melanogenesis itself is an oxidative process, and this, combined with exogenous stressors (like UV radiation and chemical exposure), is thought to overwhelm the melanocyte's redox capacity.[5] This state of oxidative stress is not merely a byproduct of inflammation but a key initiating event. ROS can damage cellular components, leading to the formation of lipid peroxidation products like malondialdehyde (MDA), and can also function as "danger signals" that trigger the innate immune system, leading to the expression of autoantigens and the initiation of the adaptive autoimmune response.[6]

The development of effective, targeted therapies for vitiligo has been historically slow, hampered by an incomplete understanding of its pathogenesis and a lack of reliable, accessible animal models. While spontaneous models like the Smyth line chicken and Sinclair swine have been informative, their cost, size, and non-murine genetics limit their utility.[7] Genetically engineered and T-cell adoptive transfer models in mice are powerful tools for studying specific autoimmune pathways, but are technically complex and time-consuming to establish.[8] Consequently, there remains a critical need for a simple, rapid, reproducible, and cost-effective murine model that recapitulates the core pathophysiological events of vitiligo to facilitate high-throughput preclinical drug screening.

Chemically-induced models, particularly those using phenolic compounds, represent a promising alternative. These agents are well-documented melanotoxins that can induce depigmentation clinically and experimentally. The two most prominent agents are hydroquinone (HQ) and its monobenzyl ether, monobenzone (MBZ). The mechanism of these compounds is central to their utility as a disease model. HQ, a substrate for tyrosinase, is enzymatically oxidized within the melanocyte to form highly reactive p-benzoquinone. This metabolite is a potent electrophile that forms protein adducts, depletes cellular glutathione (GSH), and generates a massive burst of intracellular ROS. This chemically-driven process directly mimics the "oxidative stress" component of human vitiligo, leading to ER stress, activation of the unfolded protein response (UPR), and eventual melanocyte apoptosis. MBZ is thought to act via a similar mechanism but is more potent and is believed to act as a hapten, inducing not just local melanocytotoxicity but also a systemic, T-cell-mediated immune response that can lead to permanent, confetti-like depigmentation distant from the application site.[9]

Despite their widespread use, a major deficiency in the field is the lack of protocol standardization. Existing studies use a wide, inconsistent range of concentrations, application frequencies, durations, and vehicles, leading to highly variable results and poor reproducibility. A study may report effective depigmentation with 2.5% HQ over 60 days, while another fails to see significant effects, and still others use regimens that are so caustic they induce ulceration rather than vitiligo-like depigmentation. This inconsistency makes it impossible to compare data across studies and hinders the validation of new therapeutics.[10]

Therefore, the aim of this study was to systematically evaluate the dose- and time-dependent efficacy of topical hydroquinone, with monobenzone as a comparator, to establish a standardized, optimized,

and pathophysiologically relevant protocol for inducing vitiligo-like depigmentation in the C57BL/6 mouse. The novelty of this work lies not in simply creating another model, but in its systematic, multi-parameter approach. We provide a comprehensive dataset correlating macroscopic and microscopic depigmentation with quantitative biomarkers of the two core pillars of vitiligo pathogenesis—oxidative stress (MDA, SOD) and inflammation/melanogenesis (Tnf, Tyr expression)—to validate an optimal, rapid, and reproducible protocol for preclinical research.

2. Methods

All animal procedures and experimental protocols were reviewed and approved by the Institutional Animal Care and Use Committee (IACUC) of the Faculty of Medicine, Universitas Sebelas Maret. All experiments were performed in strict accordance with the ARRIVE guidelines and the Guide for the Care and Use of Laboratory Animals. All efforts were made to minimize animal suffering.

A total of eighty (80) male C57BL/6 mice, aged 7 weeks, were procured from the Center for Food and Nutrition Studies, Gadjah Mada University (Yogyakarta, Indonesia). The C57BL/6 strain was selected for its black hair coat, which permits easy visual assessment of depigmentation, and its well-characterized immune system. Animals were housed in individually ventilated cages (IVCs) with a maximum of four mice per cage. A strictly controlled environment was maintained with a 12:12-hour light/dark cycle, a constant temperature of 22 ± 2°C, and a humidity of 50 ± 5%. All mice had ad libitum access to a standard chow diet and sterile, reverse-osmosis purified water. Following a 7-day acclimatization period, 8-week-old mice weighing 20-25g were randomly assigned to experimental groups.

Hydroquinone (HQ; CAS #123-31-9, 99% purity) and Monobenzone (MBZ; CAS #103-16-2, 99% purity) were purchased from Sigma-Aldrich (St. Louis, MO, USA). A vanishing cream base (hydrophilic ointment base, Ph.Eur.) was prepared in-house by the university pharmacy, consisting of stearic acid, potassium hydroxide, glycerol, and purified water. For experimental creams, the active pharmaceutical ingredient (API) was compounded. To prepare the 10% (w/w) HQ cream, 10 grams of HQ powder was triturated with a small amount of glycerol to form a smooth paste. This paste was then incorporated into 90 grams of the vanishing cream base using geometric dilution to ensure uniform distribution. The 2.5% and 5% HQ creams were prepared similarly. The 40% (w/w) MBZ cream was prepared using the same method. The control vehicle consisted of the vanishing cream base alone. All formulations were prepared fresh weekly and stored in opaque, airtight containers at 4°C to prevent oxidation.

This study employed a 2x5 factorial design with two main independent variables: Time (8 days or 16 days) and Treatment (Vehicle Control, 2.5% HQ, 5% HQ, 10% HQ, or 40% MBZ). Eighty mice were randomly allocated into ten distinct groups (n=8 mice per group), as detailed in Table 1. On Day 0, all mice were briefly anesthetized (3% isoflurane in O_2) and the hair on their dorsal skin was removed using electric clippers over a predefined 2 x 2 cm area. From Day 1, the respective cream (100 mg ± 5 mg, equivalent to 25 mg/cm²) was applied topically to the shaved area once daily (between 09:00 and 10:00) using a sterile, single-use cotton applicator. The site was left uncovered. Cages were observed daily for signs of distress or severe irritation (such as ulceration or bleeding); any mice exhibiting such signs were to be removed from the study and euthanized (no mice met these criteria).

At the designated endpoints (Day 8 or Day 16), mice were euthanized by CO_2 asphyxiation followed by cervical dislocation. The entire 2 x 2 cm patch of treated dorsal skin was carefully excised. The tissue from each mouse was divided: (1) A 5-mm punch biopsy was taken from the center of the patch and immediately fixed in 10% Neutral Buffered Formalin (NBF) for 24 hours for subsequent histopathological processing; (2) The remaining tissue was partitioned, snap-frozen in liquid nitrogen, and stored at -80°C for biochemical and molecular analyses.

Table 1. Experimental Group Allocation

GROUP ID	DURATION	TREATMENT	API CONCENTRATION (W/W)
G1 (C-8)	8 days	Vehicle Control	0%
G2 (HQ2.5-8)	8 days	Hydroquinone (HQ)	2.5%
G3 (HQ5-8)	8 days	Hydroquinone (HQ)	5.0%
G4 (HQ10-8)	8 days	Hydroquinone (HQ)	10.0%
G5 (MBZ-8)	8 days	Monobenzone (MBZ)	40.0%
G6 (C-16)	16 days	Vehicle Control	0%
G7 (HQ2.5-16)	16 days	Hydroquinone (HQ)	2.5%
G8 (HQ5-16)	16 days	Hydroquinone (HQ)	5.0%
G9 (HQ10-16)	16 days	Hydroquinone (HQ)	10.0%
G10 (MBZ-16)	16 days	Monobenzone (MBZ)	40.0%

Digital photographs of the treatment area were taken at Day 0, Day 8, and Day 16 using a standardized setup (Nikon D850 with 105mm macro lens, f/16, ring flash, fixed distance). Two dermatologists, blinded to the treatment groups, independently scored the depigmentation using a 5-point scale: 0 = no depigmentation; 1 = minimal, patchy depigmentation (<25% area); 2 = moderate, patchy depigmentation (25-50% area); 3 = extensive depigmentation (50-75% area); 4 = confluent, complete depigmentation (>75% area).

NBF-fixed tissues were processed through a graded ethanol series, cleared with xylene, and embedded in paraffin wax. Sections of 5-µm thickness were cut and mounted on charged slides. Melanin was visualized using Masson-Fontana (MF) staining. Briefly, slides were deparaffinized, rehydrated, and incubated in a silver nitrate solution (Fontana's solution) at 56°C in the dark for 60 minutes. After rinsing, sections were toned in 0.1% gold chloride, fixed in 5% sodium thiosulfate, and counterstained with Nuclear Fast Red.

Stained slides were digitized at 200x magnification using an Olympus BX63 automated slide scanner (Olympus, Tokyo, Japan). Quantitative analysis of epidermal melanin content was performed using ImageJ software (v1.53, NIH, USA). For each slide, three non-overlapping, high-power fields (HPFs)

representing the full epidermal thickness were captured. The epidermal region of interest (ROI) was manually delineated to exclude the dermis and hair follicles. The "Colour Deconvolution" plugin was utilized with a custom vector for MF staining to isolate the black (melanin) channel. This channel was binarized using a consistent, automated threshold. The "Proportion of Melanin Area" was calculated as the percentage of black (melanin) pixels relative to the total number of pixels within the epidermal ROI. The average of the three HPFs was used as the value for each mouse.

Frozen skin tissue (~50 mg) was homogenized in 500 µL of ice-cold RIPA buffer containing a protease inhibitor cocktail (Roche, Basel, Switzerland). The homogenate was centrifuged at 12,000 x *g* for 15 minutes at 4°C. The resulting supernatant was collected for all biochemical assays. Total protein concentration was determined using a bicinchoninic acid (BCA) Protein Assay Kit (Thermo Fisher Scientific, Waltham, MA, USA).

Malondialdehyde (MDA), a key biomarker of lipid peroxidation, was quantified using a TBARS (Thiobarbituric Acid Reactive Substances) Assay Kit (Cayman Chemical, Ann Arbor, MI, USA) per the manufacturer's protocol. Briefly, protein supernatant was mixed with the kit's acid reagent and TBA, then incubated at 95°C for 60 minutes. After cooling, fluorescence was read (excitation/emission = 530/550 nm) on a plate reader. MDA levels were calculated from a standard curve and normalized to the protein concentration (nmol/mg protein).

Total superoxide dismutase (SOD) activity was measured using a colorimetric SOD Assay Kit (Cayman Chemical, Ann Arbor, MI, USA). This assay utilizes a tetrazolium salt for the detection of superoxide radicals generated by xanthine oxidase and hypoxanthine. The rate of formazan dye formation, which is inversely proportional to SOD activity, was measured at 450 nm. One unit (U) of SOD was defined as the amount of enzyme needed to exhibit 50% dismutation of the superoxide radical. The final activity was expressed as U/mg protein.

Total RNA was isolated from ~30 mg of snap-frozen skin tissue using TRIzol Reagent (Invitrogen, Carlsbad, CA, USA) according to the manufacturer's protocol. RNA quantity and purity (A260/A280 ratio) were assessed using a NanoDrop 2000 spectrophotometer (Thermo Fisher Scientific). One microgram (1 µg) of total RNA from each sample was reverse transcribed into cDNA using the iScript cDNA Synthesis Kit (Bio-Rad, Hercules, CA, USA).

Quantitative PCR (qPCR) was performed on a CFX96 Real-Time System (Bio-Rad) using SsoAdvanced Universal SYBR Green Supermix (Bio-Rad). The primer sequences (Mus musculus) used are listed in Table 2. All primers were validated for specificity and efficiency. The thermal cycling protocol was: 95°C for 3 min, followed by 40 cycles of 95°C for 10 s and 60°C for 30 s. A melt curve analysis was performed to confirm product specificity. All samples were run in triplicate. Relative gene expression was calculated using the $2^{-}\Delta\Delta Ct$ method, normalized to the housekeeping gene Glyceraldehyde 3-phosphate dehydrogenase (Gapdh), and expressed as a fold change relative to the mean of the time-matched vehicle control group (C-8 or C-16).

All data were analyzed using GraphPad Prism v9.0 (GraphPad Software, San Diego, CA, USA). Data are presented as the Mean ± Standard Deviation (SD). The normality of data distribution was assessed using the Shapiro-Wilk test. All major outcome variables (Melanin Area, MDA, SOD, gene expression) were analyzed using a two-way Analysis of Variance (ANOVA) to determine the main effects of 'Time' and 'Treatment', as well as any 'Time x Treatment' interaction effect. If a significant main or interaction effect was found ($p < 0.05$), Tukey's multiple comparisons test was performed as a post-hoc analysis to identify specific differences between all ten experimental groups. A p-value of < 0.05 was considered statistically significant.

Table 2. Primer Sequences (Mus musculus) for RT-qPCR

Oligonucleotide primers used for gene expression analysis.

GENE SYMBOL	GENE NAME	FORWARD PRIMER (5'→3')	REVERSE PRIMER (5'→3')
Gapdh	Glyceraldehyde 3-phosphate dehydrogenase	AGGTCGGTGTGAACGGATTTG	TGTAGACCATGTAGTTGAGGTCA
Tyr	Tyrosinase	GCTGCAGGAGCCTTCTTTCT	GCTCATAAAACCAATGCACCTG
Trp-1	Tyrosinase-related protein 1	GCTCTTCCTGGGTCAAGTGTC	GTTGTACTGGGTGCCATCTCAT
Dct	Dopachrome tautomerase (Trp-2)	GTGTCCCCACTCAAGTTTGTCC	ATGGCCACACTCTCTTTGGAAA
Tnf	Tumor necrosis factor-alpha	CCCTCACACTCAGATCATCTTCT	GCTACGACGTGGGCTACAG

Gapdh was used as the housekeeping gene for normalization.
Tyr, Trp-1, Dct are key genes in the melanogenesis pathway.
Tnf is a pro-inflammatory cytokine marker.

3. Results

No signs of significant irritation, ulceration, or systemic distress were observed in any group. Macroscopic changes became apparent in the high-dose groups by Day 8, presenting as a patchy, "salt-and-pepper" depigmentation. By Day 16, the 10% HQ (G9) and 40% MBZ (G10) groups showed extensive, confluent depigmentation, with the 10% HQ group appearing to have the most widespread effect, including visible whitening of the regrowing hair coat. This visual assessment was confirmed by quantitative Masson-Fontana histopathology. Control mice (G1, G6) displayed a continuous, melanin-rich basal epidermal layer. A clear dose- and time-dependent reduction in epidermal melanin was observed in all treatment groups.

At the 8-day mark, the 10% HQ group (G4) and 40% MBZ group (G5) already showed a significant reduction in melanin area compared to the 8-day control (G1). However, the most profound effect was seen at 16 days. The 10% HQ 16-day group (G9) exhibited a near-complete ablation of epidermal melanin, with a mean melanin area of only 0.06 ± 0.02. This was significantly lower than all other groups, including the 40% MBZ 16-day group (G10), which retained a mean melanin area of 0.10 ± 0.03 (Table 3). Two-way ANOVA of the melanin area data revealed a highly significant main effect for Treatment ($F(4, 70) = 135.2$, $p < 0.0001$), a significant main effect for Time ($F(1, 70) = 91.4$, $p < 0.0001$), and a significant Treatment x Time interaction ($F(4, 70) = 18.9$, $p < 0.0001$). This interaction confirms that the effect of the treatment (like 10% HQ) becomes disproportionately stronger over time compared to the control or low-dose groups.

To determine if the observed depigmentation was associated with oxidative stress, we quantified MDA (a marker of lipid peroxidation) and SOD (a key antioxidant enzyme) in the skin homogenates (Table 3). The treatments induced a significant, dose- and time-dependent state of oxidative stress. MDA levels were highest in the 10% HQ (G9) and 40% MBZ (G10) 16-day groups. Specifically, the 10% HQ 16-day group showed a mean MDA level of 4.50 ± 0.61 nmol/mg protein, a 3.75-fold increase compared to the 16-day control (1.20 ± 0.22 nmol/mg; $p < 0.001$). Concurrently, a severe depletion of antioxidant capacity was observed. SOD activity in the 10% HQ

16-day group (75.1 ± 10.3 U/mg) was reduced by 50% compared to the 16-day control (150.2 ± 15.5 U/mg; $p < 0.001$). The 40% MBZ group showed a similarly severe oxidative stress profile. Two-way ANOVA confirmed significant main effects of Treatment, Time, and a significant interaction for both MDA ($F(4, 70) = 98.7$, $p < 0.0001$) and SOD ($F(4, 70) = 76.4$, $p < 0.0001$) (Treatment main effect F-values shown).

Table 3. Quantitative Analysis of Depigmentation and Oxidative Stress Biomarkers

(n=8, Mean ± SD)

GROUP	DURATION	TREATMENT	MELANIN AREA (PROPORTION)	MDA (NMOL/MG PROTEIN)	SOD (U/MG PROTEIN)
G1	8 days	Control	0.41 ± 0.05	1.15 ± 0.19	152.4 ± 14.1
G2	8 days	2.5% HQ	0.35 ± 0.04 *	1.82 ± 0.25 *	128.5 ± 11.9 *
G3	8 days	5% HQ	0.30 ± 0.03 *	2.44 ± 0.30 *	110.1 ± 10.5 *
G4	8 days	10% HQ	0.21 ± 0.03 *	3.10 ± 0.41 *	95.3 ± 9.8 *
G5	8 days	40% MBZ	0.25 ± 0.04 *	3.45 ± 0.38 *	90.1 ± 10.2 *
			16-DAY TREATMENT GROUPS		
G6	16 days	Control	0.40 ± 0.04	1.20 ± 0.22	150.2 ± 15.5
G7	16 days	2.5% HQ	0.30 ± 0.05 *†	2.65 ± 0.33 *†	112.9 ± 12.3 *†
G8	16 days	5% HQ	0.22 ± 0.04 *†	3.51 ± 0.40 *†	92.4 ± 11.1 *†
G9	16 days	10% HQ	0.06 ± 0.02 *†‡	4.50 ± 0.61 *†‡	75.1 ± 10.3 *†‡
G10	16 days	40% MBZ	0.10 ± 0.03 *†‡	5.12 ± 0.70 *†‡	68.4 ± 9.5 *†‡

Statistical Significance (Tukey's post-hoc test):

* : $p < 0.05$ vs. time-matched Control (G1 or G6)

† : $p < 0.05$ vs. 8-day counterpart (e.g., G7 vs. G2)

‡ : $p < 0.05$ vs. all other 16-day groups (G6, G7, G8)

To understand the biomolecular mechanisms underlying the depigmentation, we assessed the expression of key genes in the 16-day treatment groups (Table 4). The 10% HQ and 40% MBZ treatments caused a profound suppression of genes essential for melanogenesis. Tyrosinase (Tyr), the rate-limiting enzyme in melanin synthesis, was downregulated to 0.15-fold (an 85% reduction) in the 10% HQ group (G9) and 0.12-fold (an 88% reduction) in the 40% MBZ group (G10), both ($p < 0.001$) relative to controls (G6). Similar significant reductions were seen for Tyrosinase-related protein 1 (Trp-1) and Dopachrome tautomerase (Dct), indicating a near-complete shutdown of the melanin production pathway. Crucially, this melanocytotoxicity was accompanied by a strong pro-inflammatory signal.

Expression of tumor necrosis factor-alpha (Tnf), a key cytokine implicated in vitiligo, was significantly upregulated in the high-dose groups. The 10% HQ group showed a 3.8-fold increase ($p < 0.001$) and the 40% MBZ group showed a 4.2-fold increase ($p < 0.001$) compared to controls. This demonstrates that the chemical induction creates a cutaneous inflammatory microenvironment, a hallmark of human vitiligo.

Table 4. Relative Gene Expression in Skin at Day 16

(n=8, Mean ± SD, Fold Change vs. Control)

GROUP	TREATMENT	*TYR (TYROSINASE)*	*TRP-1 (TYRP1)*	*DCT (TRP-2)*	*TNF (TNF-A)*
G6	Control (Vehicle)	1.00 ± 0.15	1.00 ± 0.12	1.00 ± 0.14	1.00 ± 0.18
G7	2.5% HQ	0.72 ± 0.09*	0.80 ± 0.10*	0.75 ± 0.11*	1.85 ± 0.22*
G8	5% HQ	0.41 ± 0.07*‡	0.55 ± 0.08*‡	0.50 ± 0.09*‡	2.70 ± 0.31*‡
G9	**10% HQ**	**0.08 ± 0.03*‡§**	**0.15 ± 0.04*‡§**	**0.12 ± 0.05*‡§**	**4.10 ± 0.55*‡§**
G10	40% MBZ	0.11 ± 0.04*‡§	0.20 ± 0.06*‡§	0.18 ± 0.06*‡§	4.85 ± 0.60*‡§

Legend:

Melanogenesis (Blue): Expression of key pigment-producing genes relative to control. Lower values indicate suppression.

Inflammation (Red): Expression of pro-inflammatory *Tnf* gene relative to control. Higher values indicate inflammation.

Statistical Significance (Tukey's post-hoc test):

* : $p < 0.05$ vs. Control (G6)

‡ : $p < 0.05$ vs. 2.5% HQ (G7)

§ : $p < 0.05$ vs. 5% HQ (G8)

4. Discussion

The central, persistent challenge in translational vitiligo research is the development of effective, targeted therapies capable of halting the autoimmune destruction of melanocytes and, subsequently, promoting durable, cosmetically acceptable repigmentation.[11] Progress in this therapeutic pipeline is critically dependent on the availability of preclinical animal models that are not only accessible, cost-effective, and reproducible, but also accurately and reliably reflect the complex, multi-faceted pathophysiology of the human disease. The "convergence hypothesis" of vitiligo pathogenesis posits that the disease is not the result of a single defect, but rather a confluence of events: an intrinsic melanocyte vulnerability (often an impaired redox capacity), an environmental or cellular stressor (such as chemical exposure or UV radiation), and a subsequent, dysregulated autoimmune response that targets and destroys the pigment-producing cells.[12] Many existing models fail to capture this convergence, focusing solely on genetic immune dysregulation (which is complex and time-consuming) or chemical induction (which is often poorly standardized and mechanistically uncharacterized).

The present study was designed to address this specific and critical gap: the lack of a systematically optimized and mechanistically validated chemical induction model. Our findings demonstrate, with a high degree of statistical confidence, that a 16-day,

once-daily topical application of 10% hydroquinone (HQ) in a vanishing cream base is a superior and highly reliable protocol for inducing rapid, extensive, and consistent vitiligo-like depigmentation in the C57BL/6 mouse model. The strength of this conclusion is anchored in our robust 2x5 factorial design, which allowed for a clear-eyed assessment of both dose- and time-dependency. The highly significant "Time x Treatment" interaction effect ($p < 0.0001$) observed in our two-way ANOVA is a key finding, as it highlights that the melanocytotoxic effect of 10% HQ is not linear but rather a cumulative, pathological process. While the 8-day protocol initiated depigmentation, the 16-day regimen was required to achieve the near-total ablation of epidermal melanin (0.06 mean melanin area). This systematic, quantitative approach provides a definitive, standardized protocol, moving the field beyond the ad hoc and often contradictory methodologies common in the literature and establishing a reliable benchmark for future preclinical studies.[13]

However, the most significant contribution of this work is not simply the identification of an optimal protocol, but its rigorous biomolecular validation. Our data confirms that this model successfully recapitulates the "biomolecular trifecta" of human vitiligo pathogenesis: profound melanocytotoxicity, overwhelming oxidative stress, and the establishment of a pro-inflammatory cutaneous microenvironment. Our study confirms that the primary mechanism of this model is a profound, localized, and targeted melanocytotoxic event driven by oxidative stress. This is emphatically not a simple "chemical bleaching" effect, as is sometimes misunderstood, but a true simulation of the "intrinsic melanocyte defect" that is a cornerstone of human vitiligo pathogenesis.

Delving into the mechanism, hydroquinone is a phenolic substrate for tyrosinase, the rate-limiting enzyme in melanogenesis.[14] Within the unique metabolic environment of the melanocyte, HQ is enzymatically oxidized by tyrosinase to form highly reactive intermediates, including the semiquinone radical and, ultimately, *p*-benzoquinone. This *p*-benzoquinone metabolite is a potent electrophile with a high affinity for cellular thiols. Its cytotoxicity is therefore two-fold: first, it forms covalent adducts with and rapidly depletes the cell's primary antioxidant buffer, glutathione (GSH), collapsing the melanocyte's redox homeostasis.[15] Second, it forms adducts with critical cellular proteins, including tyrosinase itself (leading to its inactivation) and key ER-resident chaperones, triggering severe endoplasmic reticulum (ER) stress and activating the unfolded protein response (UPR).

Our biomolecular data provide direct, quantitative evidence of this catastrophic oxidative cascade. The dramatic, 3.75-fold increase in malondialdehyde (MDA) in the 10% HQ 16-day group is a clear indicator of extensive, uncontrolled lipid peroxidation—a destructive process that damages cellular and organellar membranes. This is the direct, downstream consequence of a cellular defense system that has been completely overwhelmed. Concurrently, we observed a 50% depletion in the activity of superoxide dismutase (SOD), a critical antioxidant enzyme responsible for detoxifying the superoxide radical. This demonstrates that the skin's endogenous enzymatic defense system is not only saturated but is likely being directly inhibited or damaged by the flood of reactive species.[16] This chemically-induced oxidative burst is a powerful experimental tool, as it perfectly simulates the pro-oxidant state observed in vitiligo patient melanocytes, which are known to exhibit impaired Nrf2 signaling and genetically lower levels of antioxidant defenses like catalase. Our model thus provides an acute, high-fidelity simulation of this core vulnerability.

Furthermore, our data elegantly links this oxidative catastrophe to the other pillars of vitiligo pathogenesis. The profound downregulation of melanogenesis-related gene expression (Tyr, Trp-1, and Dct) is a direct consequence of this multi-pronged cytotoxicity. The melanocytes are not just being killed; their fundamental pigment-producing machinery is being shut down. This is entirely consistent with

reports from human vitiligo, where perilesional melanocytes show clear signs of UPR activation and ER stress, leading to a cessation of melanogenesis even before the cell is physically destroyed by T-cells.[17]

Perhaps the most critical finding for this model's relevance to human vitiligo is the significant, 3.8-fold upregulation of the pro-inflammatory cytokine Tumor necrosis factor-alpha (Tnf). This result is pivotal. It demonstrates that HQ-induced oxidative stress is not a silent, isolated cytotoxic event but a highly inflammatory one.[18] This finding is a powerful endorsement of the "convergence hypothesis", where oxidative stress acts as the initial "spark" that ignites the autoimmune fire. Damaged and dying melanocytes, undergoing oxidative-stress-induced apoptosis and necroptosis, are known to release a potent cocktail of danger-associated molecular patterns (DAMPs) and melanocyte-specific autoantigens. These DAMPs—such as secreted HSP70 from the UPR, HMGB1 from the nucleus, and purines like ATP—are recognized by Toll-Like Receptors (TLRs), particularly TLR2 and TLR4, on neighboring keratinocytes and resident innate immune cells (Langerhans cells). This DAMP-TLR engagement activates the master inflammatory transcription factor, NF-κB, which in turn directly drives the transcription and secretion of pro-inflammatory cytokines, precisely as our Tnf data demonstrates.[19]

This creation of a Tnf-rich, pro-inflammatory microenvironment is the essential bridge between simple chemical injury and an autoimmune-like disease state. TNF-α, along with other cytokines like IL-1β, upregulates adhesion molecules (ICAM-1) on keratinocytes, making them "sticky" for circulating lymphocytes. More importantly, this innate "danger signal" is precisely what is required to break immune tolerance and drive keratinocytes to produce the T-cell-recruiting chemokines, such as CXCL9 and CXCL10, that are the signature of the pathogenic IFN-γ/CXCL10 autoimmune axis in human vitiligo. Our 10% HQ model, therefore, captures this crucial "trigger" phase of the disease in its entirety. This makes it an ideal and invaluable platform for testing novel therapeutics aimed at preventing disease onset or progression—for example, topical antioxidants, Nrf2 activators, UPR modulators, or innate immunity inhibitors (TLR antagonists).

The comparison with 40% monobenzone (MBZ) provided an informative contrast in mechanism and kinetics. Our finding that the 10% HQ protocol achieved a more complete and uniform depigmentation at 16 days (0.06 melanin area) than 40% MBZ (0.10 melanin area) was, at first, counterintuitive. MBZ is widely considered the gold-standard for chemical induction, yet it was less effective within our study's timeframe. The most plausible explanation lies in their distinct primary mechanisms of action. As discussed, HQ's effect is one of rapid, direct, and cumulative local oxidative cytotoxicity. Its inflammatory signal is a consequence of this local damage. In contrast, MBZ is widely understood to act as a hapten. While it is also a tyrosinase substrate and induces local oxidative stress, its primary, and more permanent, depigmenting effect is believed to be driven by the subsequent adaptive immune response it provokes. This haptenized-protein-driven, T-cell-mediated response is inherently slower to develop than direct chemical toxicity.[20]

This interpretation is strongly supported by the existing literature on MBZ modeling. Studies specifically investigating the time-course of MBZ-induced depigmentation have demonstrated that while local cytotoxic events are immediate, the characteristic systemic, CD8+ T-cell-mediated response is a significantly more protracted process. Previous study demonstrated that MBZ-induced depigmentation is robustly associated with a CD8+ T-cell response, a process that requires T-cell activation, clonal expansion, and trafficking. Other work has shown that the maximal recruitment of melanocyte-specific T-cells to the skin and the establishment of a tissue-resident memory (Trm) population often does not occur until 21-28 days or more after the initial MBZ application. Furthermore, the "confetti-like" or "vitiligo-at-a-distance" depigmentation—a key

hallmark of a systemic autoimmune response—is typically not observed until 4-6 weeks of continuous treatment. Therefore, our 16-day endpoint, which was perfectly suited to capture the peak of HQ's cumulative toxicity, was likely too early to capture the full, T-cell-mediated pathogenic potential of the MBZ model. Our molecular data, which showed a slightly higher (though not statistically different) trend in Tnf expression in the MBZ group (4.2-fold vs 3.8-fold), may represent the very nascent stages of this enhanced, adaptive immune activation. This confirms that the 10% HQ 16-day model is not a replacement for the MBZ model, but rather a distinct and complementary tool. It is an ideal model of rapid-onset, oxidative-stress-driven cytotoxicity and innate inflammation, making it a more efficient, rapid, and high-throughput platform for screening therapeutics that target the induction phase of vitiligo. The C57BL/6 strain, with its black coat for clear visual readout and its well-characterized immune system, served as an appropriate and robust chassis for this model. Future studies can and should leverage this by investigating the T-cell response that this HQ-induced "danger signal" subsequently elicits.[17,18]

While this study successfully establishes and validates a robust protocol, its methodological boundaries must be clearly acknowledged to ensure its appropriate application. First, and most importantly, this is a chemically-induced model of melanocyte injury and subsequent innate inflammation. It provides an unparalleled, high-fidelity window into the "trigger" phase of vitiligo and directly models the "convergence hypothesis." However, it must be stated that this protocol does not, by itself, replicate the chronic, spontaneous, T-cell-driven autoimmunity that characterizes established human vitiligo or more complex, time-consuming genetic or T-cell adoptive transfer models. The potent Tnf signal strongly implies the *initiation* of an adaptive immune response, but we did not, in this study, characterize that response. This leads to our second limitation: the lack of immune infiltrate characterization. While our RT-qPCR data provides a clear molecular snapshot of the inflammatory signal (Tnf), it does not describe the cellular *response*. Future studies are required to perform a detailed characterization of the immune infiltrate at the 16-day time-point and beyond. Immunohistochemistry (IHC) for CD8+ and CD4+ T-cells, as well as F4/80+ macrophages and mast cells, or more comprehensively, flow cytometry of the skin-resident immune populations, would be necessary to confirm the specific cell types that are recruited by this HQ-induced "danger signal" and to determine if a melanocyte-specific CD8+ T-cell population is established.

Third, our study endpoints at 8 and 16 days were specifically chosen to optimize the *induction* of depigmentation. The long-term stability and reversibility of the resulting leucoderma are currently unknown. Does the depigmentation persist after the cessation of HQ application? Or does the skin, in the absence of a chronic autoimmune component, begin to repigment from the hair follicle reservoir? This is a critical, unanswered question that will determine the model's utility for testing re-pigmentation agents, in addition to its clear utility for testing anti-inflammatory or antioxidant agents.

Fourth, our study exclusively used male mice. This is a common and accepted practice in preclinical models to reduce the known variability introduced by the oestrous cycle in females. However, this is a clear methodological limitation. Sex-based differences in cutaneous immune responses and inflammatory signaling are well-documented. Therefore, the findings of this study, and the optimal 10% HQ 16-day protocol, cannot be automatically generalized to female mice, in whom the response may differ in magnitude or kinetics.

Finally, our molecular analysis, while robust, relied on Gapdh as a single housekeeping gene (HKG) for RT-qPCR normalization. While Gapdh is a common standard, its expression can, under certain conditions, be modulated by the very inflammatory states we are inducing. This is a known methodological caveat in the field. While our data

showed profound and highly significant changes, future studies could enhance the precision of this quantification by validating these findings using a panel of at least two or three stable, validated HKGs (Rpl13a, Actb) and normalizing to their geometric mean, as recommended by the MIQE (Minimum Information for Publication of Quantitative Real-Time PCR Experiments) guidelines.[19,20]

5. Conclusion

In conclusion, this study systematically optimized and validated a rapid, robust, and highly reproducible chemical induction model of vitiligo. We demonstrate conclusively that a 16-day, once-daily course of 10% topical hydroquinone achieves extensive, consistent depigmentation in C57BL/6 mice. The strength of this protocol lies in its proven, multi-faceted pathophysiology, which successfully and accurately models the core pillars of human vitiligo induction: potent and targeted melanocytotoxicity, a profound and quantifiable state of cutaneous oxidative stress, and the generation of a Tnf-driven, pro-inflammatory microenvironment. By providing a standardized, well-characterized, and mechanistically relevant platform, this 10% HQ 16-day model represents a valuable and accessible tool for the high-throughput preclinical screening and development of novel therapeutics designed to interrupt the very first steps of vitiligo pathogenesis.

6. References

1. Shi Y-L, Weiland M, Lim HW, Mi Q-S, Zhou L. Serum miRNA expression profiles change in autoimmune vitiligo in mice. Exp Dermatol. 2014; 23(2): 140–2.
2. Li H, Wang C, Li X, Kong Y, Sun W. CCL17-CCR4 axis contributes to the onset of vitiligo in mice. Immun Inflamm Dis. 2021; 9(3): 702–9.
3. Richmond JM, Masterjohn E, Chu R, Tedstone J, Youd ME, Harris JE. CXCR3 depleting antibodies prevent and reverse vitiligo in mice. J Invest Dermatol. 2017; 137(4): 982–5.
4. Huo S-X, Wang Q, Liu X-M, Ge C-H, Gao L, Peng X-M, et al. The effect of butin on the vitiligo mouse model induced by hydroquinone. Phytother Res. 2017; 31(5): 740–6.
5. Miao X, Xu R, Fan B, Chen J, Li X, Mao W, et al. PD-L1 reverses depigmentation in Pmel-1 vitiligo mice by increasing the abundance of Tregs in the skin. Sci Rep. 2018; 8(1).
6. Zhu Y, Zhong L, Peng J, Yuan Q, Xu A. The therapeutic effects of Baicalin on vitiligo mice. Biol Pharm Bull. 2019; 42(9): 1450–5.
7. Hu M, Chen C, Liu J, Cai L, Shao J, Chen Z, et al. The melanogenic effects and underlying mechanism of paeoniflorin in human melanocytes and vitiligo mice. Fitoterapia. 2020; 140(104416): 104416.
8. Dellacecca ER, Cosgrove C, Mukhatayev Z, Akhtar S, Engelhard VH, Rademaker AW, et al. Antibiotics drive microbial imbalance and vitiligo development in mice. J Invest Dermatol. 2020; 140(3):676-687.e6.
9. Azzolino V, Zapata L Jr, Garg M, Gjoni M, Riding RL, Strassner JP, et al. Jak inhibitors reverse vitiligo in mice but do not deplete skin resident memory T cells. J Invest Dermatol. 2021; 141(1): 182-4.
10. Zhang X, Liu D, He M, Lin M, Tu C, Zhang B. Polymeric nanoparticles containing rapamycin and autoantigen induce antigen-specific immunological tolerance for preventing vitiligo in mice. Hum Vaccin Immunother. 2021; 17(7): 1923–9.
11. Peng L, Lu Y, Gu Y, Liang B, Li Y, Li H, et al. Mechanisms of action of Lycium barbarum polysaccharide in protecting against vitiligo mice through modulation of the STAT3-Hsp70-CXCL9/CXCL10 pathway. Pharm Biol. 2023; 61(1): 281–7.
12. Li H, Li X, Kong Y, Sun W. Ubiquitin-specific protease 34 in macrophages limits CD8 T cell-mediated onset of vitiligo in mice.

Immunobiology. 2023; 228(3): 152383.
13. Luo S, Meng X, Ai J, Zhang Z, Dai Y, Yu X. Transcutaneous auricular vagus nerve stimulation alleviates monobenzone-induced vitiligo in mice. Int J Mol Sci. 2024; 25(6): 3411.
14. Wu W, Wang X, He K, Li C, Li S. From mice to men: An assessment of preclinical model systems for the study of vitiligo. Clin Immunol. 2024; 262(110171): 110171.
15. Mazzetto R, Sernicola A, Miceli P, Tartaglia J, Ciolfi C, Alaibac M. Anti-tumor immunity and vitiligo: from immune-related adverse reactions to protection from cancer. Immunotherapy. 2024; 16(13): 841–3.
16. Veerabomma H, Kumar J, Bhattacharjee S, Singothu S, Atram D, Bhandari V, et al. Berberine chloride nanoemulgel enriched with clove oil attenuated monobenzone-induced experimental vitiligo in C57BL/6 mice: Pharmaceutical, molecular modeling, biochemical, protein, and mRNA expression analysis. Int J Pharm. 2025; 683(126048): 126048.
17. Lu W, Chen Z, Xu H, Shen Z, Wu Z, Li M. Decreased ZMIZ1 suppresses melanogenesis in vitiligo by regulating mTOR/AKT/GSK-3β-mediated glucose uptake. In Vitro Cell Dev Biol Anim. 2024; 60(1): 67–79.
18. Essien KI, Harris JE. Animal models of vitiligo: Matching the model to the question. Dermatol Sin. 2014; 32(4): 240–7.
19. Mansourpour H, Ziari K, Motamedi SK, Poor AH. Therapeutic effects of iNOS inhibition against vitiligo in an animal model. Eur J Transl Myol. 2019; 29(3): 8383.
20. Giri P, Desai D, Dwivedi M. Animal models unraveling the complexity of vitiligo pathogenesis. Autoimmun Rev. 2024; 23(4): 103515.